Robustness of the BMP Morphogen Gradient in Drosophila embryonic patterning Supplementary Information

Avigdor Eldar*, Ruslan Dorfman*, Daniel Weiss*, Hilary Ashe[%], Ben-Zion Shilo* and Naama Barkai*[#]

Departments of Molecular Genetics and Physics of Complex Systems[#]*
Weizmann Institute of Science
Rehovot, Israel

[%] *School for Biological Sciences, University of Manchester*
Manchester M13 9PT , UK

Contents

1 The full patterning system

1.1 Notation

For simplicity, the following single-letter notation are used in the analysis below:

Substance	Short notation	Notation in the paper
Sog	s	$[sog]$
Scw	s_c	$[scw]$
Tld	T	$[tld]$
Scw Receptor (Sax)	r_1	
Tsg	t_{sg}	
Dpp	d_p	
Dpp Receptor (Tkv)	r_2	
Scw-receptor complex	$\{r_1 s_c\}$	
Dpp-receptor complex	$\{r_2 d_p\}$	
Sog-Scw complex	c_1	
Sog-Tsg complex	s_2	
Sog-Tsg-Dpp complex	c_2	
Average Scw concentration	$\overline{s_c}$	$[scw]_{ave}$
Average Dpp Concentration	$\overline{d_{pp}}$	
Total sax concentration	r_1^{tot}	
Total tkv concentration	r_2^{tot}	

Rate constants are as defined in main text.

1.2 model equations

The full model results presented in the paper's figure 3, was obtained by numeric simulation of the following system of equations:

$$\frac{\partial s}{\partial t} = D_s \nabla^2 s - k_b^{(1)} s s_c - k_{br}^{(1)} s\{r_1 s_c\} - \alpha t_{sg} s + \eta_s(x) \tag{1a}$$

$$\frac{\partial c_1}{\partial t} = D_{c1} \nabla^2 c_1 + k_b^{(1)} s s_c + k_{br}^{(1)} s\{r_1 s_c\} - \lambda_1 T(x) c_1 \tag{1b}$$

$$\frac{\partial s_c}{\partial t} = -k_b^{(1)} s s_c - k_r^{(1)} s_c r_1 + \lambda_1 T(x) c_1 + \eta_{sc}(t) \tag{1c}$$

$$\frac{\partial \{r_1 s_c\}}{\partial t} = -k_{br}^{(1)} s\{r_1 s_c\} + k_r^{(1)} s_c r_1 \tag{1d}$$

$$r_1^{tot} = r_1 + \{r_1 s_c\} \tag{1e}$$

$$\frac{\partial t_{sg}}{\partial t} = D_{tsg} \nabla^2 t_{sg} - \alpha t_{sg} s + \lambda_2 T(x) c_2 \tag{1f}$$

$$\frac{\partial s_2}{\partial t} = D_{s2} \nabla^2 s_2 - k_b^{(2)} s_2 d_p - k_{br}^{(2)} s_2\{r_2 d_p\} + \alpha t_{sg} s \tag{1g}$$

$$\frac{\partial c_2}{\partial t} = D_{c2} \nabla^2 c_2 + k_b^{(2)} s_2 d_p + k_{br}^{(2)} s_2\{r_2 d_p\} - \lambda_2 T(x) c_2 \tag{1h}$$

$$\frac{\partial d_p}{\partial t} = -k_b^{(2)} s_2 d_p - k_r^{(2)} d_p r_2 + \lambda_2 T(x) c_2 + \eta_{dpp}(t) \tag{1i}$$

$$\frac{\partial \{r_2 d_p\}}{\partial t} = -k_{br}^{(2)} s_2\{r_2 d_p\} + k_r^{(2)} r_2 d_p \tag{1j}$$

$$r_2^{tot} = r_2 + \{r_2 d_p\} \tag{1k}$$

The equations were solved on a ring of circumference L with $x = 0$ at the dorsal midline. In addition to the reactions described in Box 1 of the paper, this model considers the interaction of Scw with its receptor and the formation of the Dpp gradient through its interaction with Sog, Tsg and Tld. The model simulates explicitly the kinetics in all regions of the embryo. Sog is produced continuously with a rate $\eta_s(x)$ in the region flanking the dorsal part ($l_1 < |x| < l_1 + l_2$), while Scw is produced at a rate η_{sc} in all parts of the embryo and Dpp is produced in the dorsal region at a rate η_{dpp}. Both Scw and Dpp are produced during a limited time ($0 < t < \tau$). $T(x)$ is non-zero, only at the dorsal ectoderm ($|x| < l_1$). The reference system was defined by the following parameters: $D_s = D_c = D_{Tsg} = D_{s2} = D_{c2} = 85\mu m^2\,\mathrm{sec}^{-1}$, $L = 550\mu m, l1 = 125\mu m, l2 = 100\mu m$, $T = 0.5\mu M$, $t_{sg} = 0.4\mu M$, $\eta_s = 0.02\mu M\,\mathrm{sec}^{-1}$; $\eta_{sc} = 0.19 nM\,\mathrm{sec}^{-1}$, $\eta_{dpp} = 0.16 nM\,\mathrm{sec}^{-1}$, $t = 600\,\mathrm{sec}$, $\alpha = 0.02\,\mathrm{sec}^{-1}\,\mu M^{-1}$, $\lambda_1 = 2\,\mathrm{sec}^{-1}\,\mu M^{-1}$, $\lambda_2 = 4\,\mathrm{sec}^{-1}\,\mu M^{-1}$. $k_b^{(1)} = k_{br}^{(1)} = 2\,\mathrm{sec}^{-1}\,\mu M^{-1}$, $k_b^{(2)} = k_{br}^{(2)} = 0.25\,\mathrm{sec}^{-1}\,\mu M^{-1}$, $k_r^{(1)} = 2\,\mathrm{sec}^{-1}\,\mu M^{-1}$, $k_r^{(2)} =$

$1\,\mathrm{sec}^{-1}\,\mu M^{-1}$, and the total receptor concentration was taken to be $r_1^{tot} = 0.25\mu M$, $r_2^{tot} = 0.1\mu M$. An arbitrary threshold representing 5% receptor occupancy for Scw and 10% for Dpp were defined. The positions where the levels of occupied receptors reached this threshold was tested for the different parameters. For the reference system, these positions are located ˜12 cells from the dorsal midline. Similar robustness is obtained for other choices of threshold.

The two models presented in figure 2a-b, are solutions of the equations presented in the method section of the paper, using the following parameters (in arbitrary units): *Non-Robust system (Fig. 2a)*: $D_s = 1, D_{scw} = 0.01$, $D_c = 0.01$, $k_b = 10$, $k_{-b} = 0.5$, $\lambda[tld] = 2$, $\alpha[tld] = 10$, $\eta_s = 10$, $scw_{av} = 1$. *Robust system (Fig 2b)*: $D_s = 1, D_{scw} = 0.01$, $D_c = 10$, $k_b = 120$, $k_{-b} = 1$, $\lambda[tld] = 200$, $\alpha[tld] = 1$, $\eta_s = 10$, $scw_{av} = 1$.

1.3 Choice of parameters

To date, no biochemical measurements are available which constrain the assignment of parameter values. For most the parameters, including production rates, binding constants and concentrations, the biological relevant range spans several orders of magnitude. Proper patterning, which reproduce the profile of the BMP signaling pathway, is obtain for a wide range of parameters values.

The parameters of the reference system are within the realistic biochemical range, and obey the robustness conditions (Eq. 24-25 below). Here we describe the rational which guided our choice of reference system

- **Length scale**. The circumference of the embryo ($550\,\mu$m), determines the system's length scale. The appropriate length for the dorsal region is $2l_1 = 250\,\mu$m and for each side of the neural ectoderm is $l_2 = 100\,\mu$m.
- **Diffusion rates**.
  - The diffusion rate determines the patterning time. J. Ross et. al. (Nature, 410 479-483) reported that wild-type embryos accumulate P-MAD in an 18–20-cell-wide dorsal stripe at mid-cellularization that rapidly resolves into an 8–9-cell-wide stripe of more intense staining, as gastrulation starts. These observations again limit the patterning time, which amounts to at least several diffusion times, to ∼20 minutes.

- *Measurement of diffusion time.* The diffusion time at the perivitilline fluid were measured by D. Stein et. al. (Cell, 65 725-735), who injected FITC-conjugated BSA into the perivitilline compartment of a recipient embryo. They observed that within 10 minutes after injection, the fluorescent material has become distributed uniformly within the perivitelline space surrounding the embryo. BSA is a 66 kDa protein. Considering the length of the embryo to be $\sim 500\,\mu$m and assuming that 10 minutes correspond to at least two diffusion times one obtains an estimation of $D \sim 10^2 - 10^3\,\mu\mathrm{m}^2\,\mathrm{sec}^{-1}$.
- It is possible that mixing processes in the perivitelline fluid contribute to the equilibration process. For simplicity we approximate such processes as an effective diffusion. This approximation does not affect our conclusions.
- The diffusion rate of the diffusing molecules in our model was chosen as the rate measured for GFP in water, $D = 85\,\mu\mathrm{m}^2\,\mathrm{sec}^{-1}$. (Swaminathan et al., 1997, Biophysical J, Vol 72, 1900-1907). The associated diffusion time scale for the system is $\tau_{diff} = 3\,\mathrm{min}$ and for the whole circumference of the embryo $\tau_{circ} \sim 20\,\mathrm{min}$. Patterning time is about $6\tau_{diff}$ for the reference parameters (see also section 5)

- **Characteristic concentrations and reaction rates**
  - *Receptor concentration.* To determine characteristic concentrations, we assume that the external cell surface facing the perivitilline space contains ~ 1000 receptors. For typical cell surface of about $10\,\mu\mathrm{m}^2$ and a perivitelline layer of $0.5\,\mu$m, this correspond to a receptor concentration of $R = 0.3\mu M$.
  - **Threshold for cell-fate determination**. We assume that the amnioserosa differentiation threshold corresponds to $\sim 10\%$ occupied receptors. From Eq. 3 in Box 1, such a threshold is realized at the position $x = l_1/3$ when $\frac{l_b^2}{l_1^2} = \frac{2D_s/l_1^2}{k_b} = 0.005\mu M$, which leads to a binding rate of Sog to Scw, $k_b = 2\mu M^{-1} sec^{-1}$.

- **Production rates**. Sog production rates in the reference system correspond to ~ 50 molecules/cell/sec.

2 Extendening the simple model

2.1 Analysis of the simplified system (Box 1)

The set of equations analysed in Box 1 of the paper includes the interaction between Scw, Sog and Tld and describes the system's kinetics in the dorsal region:

$$\frac{\partial s}{\partial t} = D_s \nabla^2 s - k_b s s_c \tag{2}$$
$$\frac{\partial c}{\partial t} = D_c \nabla^2 c + k_b s s_c - \lambda T c \tag{3}$$
$$\frac{\partial s_c}{\partial t} = -k_b s s_c + \lambda T c. \tag{4}$$

The steady state solution is derived by setting the LHS of the above equations to zero, and is defined by the following three equations:

$$D_s \nabla^2 s = k_b s s_c \tag{5}$$
$$D_c \nabla^2 c = \lambda T c - k_b s s_c \tag{6}$$
$$k_b s s_c = \lambda T c. \tag{7}$$

Substituting Eq. 4 into Eqs 3 and 2, we obtain:

$$D_s \nabla^2 s = \lambda T c \tag{8}$$
$$D_c \nabla^2 c = 0 \tag{9}$$
$$s_c = \frac{\lambda T c}{k_b s}. \tag{10}$$

The general solution to Eq. 9 is given by:

$$c = c_0 + \sigma x. \tag{11}$$

However, from the symmetry of the system we know that $c(x) = c(-x)$, implying that $\sigma = 0$. Thus, the complex level is uniform,

$$c = c_0. \tag{12}$$

Substituting Eq. 10 into Eq. 8 we obtain:

$$D_s \nabla^2 \frac{\lambda T c}{k_b s_c} = \lambda T c, \tag{13}$$

since the complex is uniform (Eq. 12), we can divide both sides of the above equation by $\lambda T c$ to obtain the effective Scw diffusion equation (Eq. 1 in Box 1):

$$\nabla^2 s_c^{-1} = \frac{k_b}{D_s} \equiv 2 l_b^{-2}. \tag{14}$$

Eq. 14 is solved by straightforward integration. Substituting the above results into Eqs. 8, we obtain:

$$c = c_0 \tag{15}$$

$$s = \frac{\lambda T c_0}{2 D_s}(x^2 + \varepsilon^2) \tag{16}$$

$$s_c = \frac{l_b^2}{x^2 + \varepsilon^2}. \tag{17}$$

The kinetics outside the dorsal region defines the boundary conditions (see section 3). In this analysis we denote the value of Sog flux at the boundary of the dorsal region by $s(x = \pm l_1) = s_0$ and the average level of Scw (averaged around the full circumference of the embryo, L) by $\overline{s_c}$. The values of c_0 and ε are determined by these boundary conditions:

$$c_0 = \frac{2 D_s}{\lambda T} \frac{s_0}{l_1^2 + \varepsilon^2} \tag{18}$$

(similarly, we can use constant Sog flux, η_s, boundary condition and find $c_0 = \frac{\eta_s / l_1}{\lambda T}$, for further discussion see section 3).

$$\overline{s_c} = c_0 + \frac{1}{L}\int_{-l_1}^{l_1} s_c dx. \tag{19}$$

Here we have assumed that s_c vanishes outside of the dorsal region. This assumption is not essential, as we show in section 3.3. Substituting the solution for s_c (Eq. 17) into Eq. 19:

$$\overline{s_c} = c_0 + \frac{1}{L}\int_{-l_1}^{l_1} \frac{l_b^2}{x^2+\varepsilon^2} dx \approx c_0 + L^{-1}\frac{\pi l_b^2}{\varepsilon}, \tag{20}$$

where we have used the approximation $\int_{-l_1}^{l_1} \frac{dx}{x^2+\varepsilon^2} \simeq \pi\varepsilon^{-1}$. This approximation is valid for $\varepsilon \ll l_1$. Under these conditions, the value of ε is given by:

$$\varepsilon = \frac{\pi l_b^2}{\overline{s_c} - c_0} L^{-1}. \tag{21}$$

Thus, the approximation $\varepsilon \ll l_1$ is indeed valid for large enough $\overline{s_c}$. For positions that are far enough from the dorsal midline, $x \gg \varepsilon$, we find that the level of Scw is given by its robust value (**Eq. 3** in box 1):

$$s_c = \frac{l_b^2}{x^2} \qquad x \gg \varepsilon. \tag{22}$$

We find Scw profile is robust to the concentrations of Sog, Scw and Tld. The only condition for robustness is that ε remains considerably small compared to the length of the dorsal domain, $l_1; \varepsilon \ll l_1$, under perturbations. This will be true if:

$$\overline{s_c} - c_0 \gg \frac{l_b^2}{l_1}. \tag{23}$$

Since the complex level, c_0, depends on s_0 and T, we further demand that its value will be negligible compared to the averaged Scw level, obtaining the robustness condition:

$$\overline{s_c} \gg c_0 = \frac{2D_s}{\lambda T}\frac{s_0}{(1+\varepsilon^2)} \approx \frac{2s_0}{\lambda T}D_s. \tag{24}$$

The first robustness condition (Eq. 23) can then be written as:

$$\overline{s_c} \gg \frac{l_b^2}{l_1}. \tag{25}$$

Eqs. 24 and 25 are the system's **robustness conditions** (see discussion on section 4).

2.2 Binding of Scw to Sax

The model simulated in the paper (Fig. 3) considers explicitly the binding of Scw to its receptor Sax (r). The output in this case is the steady state concentration of receptor-bound Scw, $\{rs_c\}$. We assume that Sog can bind Scw even when the latter is bound to its receptor. Robustness to the level of receptors is crucially dependent on this assumption. In the dorsal region, the model is defined by the following set of equations:

$$\frac{\partial s}{\partial t} = D_s\nabla^2 s - k_b s s_c - k_{br} s\{rs_c\} \tag{26}$$

$$\frac{\partial c}{\partial t} = D_c\nabla^2 c + k_b s s_c + k_{br} s\{rs_c\} - \lambda T c \tag{27}$$

$$\frac{\partial s_c}{\partial t} = -k_b s s_c - k_r s_c r + \lambda T c \tag{28}$$

$$\frac{\partial\{r_1 s_c\}}{\partial t} = -k_{br} s\{rs_c\} + k_r s_c r \tag{29}$$

$$r^{tot} = r + \{rs_c\}, \tag{30}$$

where r^{tot} denotes the total concentration of receptors (which is assumed to be constant and uniform). Adding Eqs. 28, 29 and defining effective Scw concentration Σ_c:

$$k_b\Sigma_c = k_b s_c + k_{br}\{rs_c\}, \tag{31}$$

we find that at steady state, the system is reduced to the simple system's set of equations, Eqs. 5-7 above:

$$0 = D_s \nabla^2 s - k_b s \Sigma_c \tag{32}$$
$$0 = D_c \nabla^2 c + k_b s \Sigma_c - \lambda T c \tag{33}$$
$$0 = -k_b s \Sigma_c + \lambda T c. \tag{34}$$

The steady state profile is given by:

$$\Sigma_c = \frac{l_b^2}{x^2 + \varepsilon^2}. \tag{35}$$

The effective Scw concentration will reach a robust profile in most of the dorsal region, $\Sigma_c = \frac{l_b^2}{x^2}$, under the robustness condition $\varepsilon \ll l_1$. The output of the system, however, is the concentration of receptor-bound Scw, which determines the activation level of the BMP pathway. The relative contributions of receptor-bound and free Scw are determined by the steady state of Eqs. 29,30:

$$rs_c = \frac{k_{-r} + k_{br} s}{k_r} \{rs_c\} \tag{36}$$
$$r + \{rs_c\} = r^{tot}, \tag{37}$$

from which we obtain:

$$s_c = \frac{k_{-r} + k_{br} s}{k_r} \frac{\{rs_c\}}{r^{tot} - \{rs_c\}}. \tag{38}$$

For $k_r r^{tot} \gg k_{-r}, k_{br} s$ most Scw will be bound to receptors, with free Scw starting to accumulate only in the region where the receptors are saturated. Using Eq. 38, and the definition of Σ_c, we find that when the robustness conditions (Eq. 24, 25 above) are satisfied, the distribution of receptor-bound Scw in the dorsal region is given by the robust profile:

$$\{rs_c\} \simeq \left\{ \begin{array}{ll} \frac{l_b^2}{x^2+\varepsilon^2} & \frac{l_{br}^2}{x^2} < r^{tot} \\ r^{tot} & \frac{l_{br}^2}{x^2} > r^{tot} \end{array} \right\}, \tag{39}$$

where $l_{br}^2 = 2D_s/k_{br}$ depends only on *fixed* parameters and not on the concentration or production rates of Sog, Scw, Tld or the receptor.

2.3 Including Dpp/Tsg

The above analysis focuses on the formation of the Scw gradient while neglecting the affects of Dpp, the second activating ligand. In this section we extend the model to include the interaction of Dpp with Sog and Tsg. Interestingly, we find that a direct interaction between Dpp and Sog renders the system non-robust to Scw levels. This is shown in detail in section 7.2 below. Robustness is retained, however, when the experimentally observed requirement for Tsg in mediating the Dpp-Sog interaction is considered. Specifically, we assume that free Sog binds Scw but does not bind Dpp. Sog, however, binds also Tsg, and the complex Sog-Tsg may then bind Dpp, but not Scw.

We find that both activation gradients (Dpp and Scw) are established independently through the shuttling mechanism described in Box 1. Tsg is crucial for decoupling the two processes; thus, while Sog is responsible for shuttling Scw, Dpp is being shuttled by the complex [Sog-Tsg]. This 'division of labor' prevents local competition between Scw and Dpp. Globally, the two ligands still compete for Sog. However, since the activation profile is robust to levels of the shuttling molecule (See above section 2.1), the ratio between free Sog and Sog-Tsg does not affect patterning. The extended model is defined by the following set of equations:

$$\frac{\partial s}{\partial t} = D_s \nabla^2 s - k_b^{(1)} s s_c - \alpha t_{sg} s \tag{40}$$

$$\frac{\partial c_1}{\partial t} = D_{c1} \nabla^2 c_1 + k_b^{(1)} s s_c - \lambda_1 T c_1 \tag{41}$$

$$\frac{\partial s_c}{\partial t} = -k_b^{(1)} s s_c + \lambda_1 T c_1 \tag{42}$$

$$\frac{\partial t_{sg}}{\partial t} = D_{Tsg} \nabla^2 t_{sg} - \alpha t_{sg} s + \lambda_2 T c_2 \tag{43}$$

$$\frac{\partial s_2}{\partial t} = D_{s2} \nabla^2 s_2 - k_b^{(2)} s_2 d_p + \alpha t_{sg} s \tag{44}$$

$$\frac{\partial c_2}{\partial t} = D_{c2} \nabla^2 c_2 + k_b^{(2)} s_2 d_p - \lambda_2 T c_2 \tag{45}$$

$$\frac{\partial d_p}{\partial t} = -k_b^{(2)} s_2 d_p + \lambda_2 T c_2. \tag{46}$$

Thus, the formation of the Dpp gradient proceeds through the mechanism described in Box 1 and section 2.1 above. The shuttling molecule here is the

Sog-Tsg complex, s_2. Note that the term $\alpha T_{sg} s$ functions as the effective source for s_2. At steady state T_{sg} is approximately uniform:

$$T_{sg}(x) \simeq \overline{T_{sg}}. \tag{47}$$

so that the s_2 source follows the Sog profile, with $\eta_{s2} = \alpha T_{sg} s$. However, since Sog profile vanishes near the dorsal midline ($x = 0$), the expression for Dpp profile is essentially the same as that of Scw (Eq. 17):

$$d_{pp} = \frac{2D_s/k_b^{(2)}}{x^2 + \varepsilon^2}. \tag{48}$$

This profile will be robust to Sog,Tld and Tsg, when the second robustness condition applies (Eq. 25):

$$c_2^0 \simeq \frac{\eta_{s2}}{\lambda_2 T} \propto \frac{T_{sg}\eta_s}{T} \ll \overline{d_{pp}}. \tag{49}$$

Experimentally, it was found that the system is not robust to the levels of Dpp (e.g. Fig. 1d in the paper). This will be the case when the Dpp levels are not sufficient to satisfy the second robustness conditions (Eq. 24),

$$\varepsilon_{dpp} \approx l_1 \Longrightarrow \overline{d_{pp}} \approx l_{b(2)}^2/l_1^2 \equiv \frac{2D_s}{k_b^{(2)}}. \tag{50}$$

2.3.1 Reaching the full set of equations

To get the full set of equations, 1a-1k, used in the numerical simulation for the system we incorporate the assumption of ligand-receptor reactions introduced in section 2.2 (equations 28-30) into the set of equations for Dpp/Scw patterning (equations 40-46 above).

3 Boundary conditions

3.1 Sog profile outside the dorsal region

The equations describing the kinetics of the system outside the dorsal region are different from those in the dorsal region in two aspects. First, Tld is not expressed outside the dorsal region and does not diffuse, so Sog is not cleaved. Second, Sog is being produced in most of this region. Using the

simple model for Scw, Sog and Tld we find the steady-state equations in the neural ectoderm to be:

$$0 = D_s \nabla^2 s - k_b s s_c + \eta_s \tag{51}$$
$$0 = D_c \nabla^2 c + k_b s s_c \tag{52}$$
$$0 = -k_b s s_c. \tag{53}$$

Eq. 53 implies that $s_c = 0$ in this region. Eq. 52 implies that the complex Scw-Sog is uniform in this region, and from continuity consideration its value is the same as in the dorsal region, $c = c_0$. Eq. 51 then turns into:

$$D_s \nabla^2 s + \eta_s = 0, \tag{54}$$

which has a solution:

$$s = s_{\max} - \frac{\eta_s}{2D_s}(x - x_0)^2. \tag{55}$$

In the mesoderm there is no Sog production or Tld cleavage so the steady state equation is $\nabla^2 s = 0$ which results in a uniform concentration $s = s_{meso}$. From continuity of the Sog concentration and flux between the neural ectoderm and the mesoderm we deduce that $s_{\max} = s_{meso}$ and $x_0 = l_1 + l_2$ (which is the boundary between the neural ectoderm and the mesoderm). From continuity consideration of Sog on the boundary between the neural ectoderm and the dorsal region we find that $s_{\max} = s_0 + \frac{\eta_s}{2D_s} l_2^2 \approx \frac{\eta_s}{2D_s}(l_1^2 + l_2^2)$, where $s_0 = \frac{\eta_s}{2D_s}(l_1^2 + \varepsilon^2)$ is the value of Sog on the dorsal region boundary.

3.2 Sog flux conservation

We can deduce the level of complex easily from consideration of total Sog flux conservation. The produced Sog flux is just:

$$F_{in} = \eta_s l_2. \tag{56}$$

The degraded Sog flux level is:

$$F_{out} = \int_0^{l_1} \lambda T c dx. \tag{57}$$

In steady state, the net fluxes should be equal:

$$\eta_s l_2 = \int_0^{l_1} \lambda T c dx = \lambda T c_0 l_1. \tag{58}$$

The complex level c_0 is:

$$c_0 = \frac{\eta_s}{\lambda T} \frac{l_2}{l_1}. \tag{59}$$

Note that the system will achieved steady state only when enough Scw is available (see section 4 for further details):

$$\bar{s}_c > c_0 = \frac{\eta_s}{\lambda T} \frac{l_2}{l_1}. \tag{60}$$

3.3 Ubiquitous expression of Tld

To assess the robustness to excess levels of Tld, we over-expressed Tld using a maternal Gal4 driver. It is important to note this experiment had affected both the concentration of Tld as well as its expression domain. While in wild-type embryos Tld expression is restricted to the dorsal domain, the Mat-Gal4 driver leads to uniform expression in all cells. We find that patterning is robust to this over-expression, indicating that the Tld restricted expression to the dorsal domain is not required for patterning.

In this section we extend the mathematical analysis of the model to account for uniform Tld distribution, and demonstrate that it does not alter the robustness of the system. Surprisingly, we show that Scw will still accumulate preferentially in the dorsal region rather then being distributed between the dorsal and the ventral regions.

We define the three different expression regions of the embryo on a circular axis; The dorsal region ($0 < |x| < l_1$), the neural ectoderm($l_1 < |x| < l_1 + l_2$) and the mesoderm ($l_1 + l_2 < |x| < l_1 + l_2 + l_3 = L/2$). The steady state equations for these regions in case of ubiquitous Tld expression are:

For the dorsal region and the mesoderm:

$$0 = D_s \nabla^2 s - k_b s s_c \tag{61}$$
$$0 = D_c \nabla^2 c + k_b s s_c - \lambda T c \tag{62}$$
$$0 = -k_b s s_c + \lambda T c. \tag{63}$$

For the neural ectoderm:

$$0 = D_s \nabla^2 s - k_b s s_c + \eta_s \tag{64}$$
$$0 = D_c \nabla^2 c + k_b s s_c - \lambda T c \tag{65}$$
$$0 = -k_b s s_c + \lambda T c. \tag{66}$$

Solving these we find for the three regions:

For the dorsal region ($x = 0$ at the dorsal midline):

$$c = c_0 \tag{67}$$
$$s = \frac{\lambda T c_0}{2 D_s}(x^2 + \varepsilon_d^2) \tag{68}$$
$$s_c = \frac{l_b^2}{x^2 + \varepsilon_d^2}. \tag{69}$$

For the neural ectoderm:

$$c = c_0 \tag{70}$$
$$s = s_{\max} - \frac{\eta_s - \lambda T c_0}{2 D_s}(x - x_0)^2 \tag{71}$$
$$s_c = \frac{\lambda T c_0}{k_b s}. \tag{72}$$

For the mesoderm ($x = L/2$ is the mesoderm center):

$$c = c_0 \tag{73}$$
$$s = \frac{\lambda T c_0}{2 D_s}((\frac{L}{2} - x)^2) + \varepsilon_m^2) \tag{74}$$
$$s_c = \frac{l_b^2}{(\frac{L}{2} - x)^2 + \varepsilon_m^2}, \tag{75}$$

where $l_b^2 = 2D_s/k_b$ and the parameters $s_{max}, x_0, \varepsilon_m, \varepsilon_d$ and c_0 are integration coefficients. These parameters are found by using the continuity conditions of Sog profile and its derivative at the regions boundaries:

$$\frac{\lambda T c_0}{D_s} l_1 = -\frac{\eta_s - \lambda T c_0}{D_s}(l_1 - x_0) \tag{76}$$

$$\frac{\lambda T c_0}{D_s} l_3 = -\frac{\eta_s - \lambda T c_0}{D_s}(l_1 + l_2 - x_0) \tag{77}$$

$$\frac{\lambda T c_0}{2D_s}(l_1^2 + \varepsilon_d^2) = s_{\max} - \frac{\eta_s - \lambda T c_0}{2D_s}(l_1 - x_0)^2 \tag{78}$$

$$\frac{\lambda T c_0}{2D_s}(l_3^2 + \varepsilon_m^2) = s_{\max} - \frac{\eta_s - \lambda T c_0}{2D_s}(l_1 + l_2 - x_0)^2. \tag{79}$$

Using Scw flux conservation (see section 3.2, but with slight difference that Tld degrades the complex everywhere this time) we find:

$$c_0 = \frac{\eta_s}{\lambda T}\frac{l_2}{L}. \tag{80}$$

dividing Eqs. 76,77 we find:

$$x_0 = \frac{L}{2}\frac{x_1}{x_1 + x_3}. \tag{81}$$

Substructing Eq. 78 from 79 and using Eqs. 80,81 we obtain a relation between the two ε's:

$$\varepsilon_d^2 - \varepsilon_m^2 = \frac{1}{2}L(l_3 - l_1). \tag{82}$$

The last equation implies that $\varepsilon_d < \varepsilon_m$, since the mesoderm is smaller than the dorsal region ($l_3 < l_1$).To account for increasing amounts of Scw it must be that, $\varepsilon_d \longrightarrow 0$, but then ε_m converges to a positive value $\varepsilon_m \longrightarrow (L(l_1 - l_3))^{1/2} > 0$. This means that the amount of Scw at the mesoderm is bounded. Scw distribution in the mesoderm will *not* exhibit the limiting profile, but reach a positive and relativly shallow peak (with $\varepsilon_m \sim l_3$). In the dorsal region, however, Scw distribution is not affected by the overexpression of Tld. The model thus accounts for the observed robustness to

uniform over-expression of Tld. We find that although ubiquitos expression of Tld renders the system a dorsal-ventral symmetry in terms of expression patterns of all components, the dorsal-ventral symmetry is broken due to the difference in size of the two regions. The larger region exhibit the limiting profile, while the smaller doesn't.

4 Robustness conditions

Robustness of Scw concentration at x_{th} , $s_c = \frac{l_b^2}{x^2+\varepsilon^2}$, is maintained as long as changes in the levels of Scw, Sog or Tld will not change the relation:

$$\varepsilon = \frac{\pi l_b^2}{\overline{s_c} - c_0} L^{-1} \ll x_{th} \sim l_1. \tag{83}$$

This condition will be achieved if the parameters follow two conditions:

$$\overline{s_c} \gg \frac{\pi l_b^2}{L x_{th}} \approx \frac{l_b^2}{l_1^2} \tag{84}$$

$$\overline{s_c} \gg c_0 \propto \frac{\eta_s}{T}. \tag{85}$$

Without the second condition, any increase in the level of c_0 will lead to the immposible situation $c_0 > \bar{s}_c$ (i.e. $\varepsilon < 0$) and to a loss of steady state (see below). We note that the first condition is relevant mostly for the robustness of the system to variations in Scw concentration, while the second is relevant mostly for robustness of the system to variations in either Sog or Tld concentration. For example, in the case of Dpp (see section 2.3), the system is robust to Sog and Tld but not Dpp, because ε is of order of the dorsal region dimensions so any change of Dpp concentration will considerably change Scw profile.On the other hand, the second inequality holds, so changes in the level of c_0 will not change much the level of ε.

We stress here the fact that the system losses its steady state solution, Eqs. 16-17, when the anticipated steady state level of the complex (either of Eqs. 59 or 18) is bigger than the total Scw concntration, $c_0 > \bar{s}_c$. In such a case, Sog will continue to accumulate indefinitely and subsequently all Scw will be bounded to Sog. Activation of the system will drop to zero. This situation is similar to a case of tld mutant phenotype.

4.1 Normalized system of equations

Robust patterning is achieved for a wide range of parameter values and in different regions of parameter space. For a better understanding of the robustness condition, it is useful to consider the dimensionless form of Eqs. 2-4. To do that, we consider the following characteristic dimensions:

Dimension	Units	Physical meaning
Length	l_1	The dorsal region half-length
Time	$l_1^2/D_s = \tau_{diff}$	Sog diffusion time across the dorsal region
Concentration	$2/(k_b\tau_{diff}) = l_b^2/l_1^2$	Scw concentration which is enough to capture Sog along the length of the dorsal region

Using these dimensions, the system's parameters are reduced to four normalized parameters:

$$s_0^* = \frac{s_0}{l_b^2/l_1^2} \qquad ,\lambda^* = \lambda T \tau_{diff} \equiv \frac{\tau_{diff}}{\tau_{tld}} \qquad ,d = \frac{D_c}{D_s} \qquad ,\bar{s}_c^* = \frac{\bar{s}_c}{l_b^2/l_1^2}. \quad (86)$$

The parameters of the reference system correspond to characteristic dimension, $l_1 = 125\,\mu$m, $\tau_{diff} \approx 3\,$min, $l_b^2/l_1^2 \approx 5nM$. The normalized parameters are; $s_0^* \simeq 3600$, $\lambda^* \simeq 180$, $d = 1$, $\bar{s}_c^* \simeq 20$.

Using the new variables and omitting the asterisk sign, Eqs. 2-4 and the boundary conditions can be written as:

$$\frac{\partial s}{\partial t} = \nabla^2 s - 2ss_c \qquad ; s(x=1) = s_0 \quad (87)$$

$$\frac{\partial c}{\partial t} = d\nabla^2 c + 2ss_c - \lambda c \quad (88)$$

$$\frac{\partial s_c}{\partial t} = -2ss_c + \lambda c \qquad \int (s_c + c)\, dx = \overline{s_c}. \quad (89)$$

The solution for the normalized equations is (for $\varepsilon \ll 1$):

$$c = c_0 \approx 2\frac{s_0}{\lambda} \quad (90)$$

$$s = \tfrac{1}{2}\lambda c_0 (x^2 + \varepsilon^2) \quad (91)$$

$$s_c = \frac{1}{x^2 + \varepsilon^2}; \qquad \varepsilon \cong \frac{\pi}{2}\bar{s}_c^{-1} \quad (92)$$

The robustness conditions are:

$$\overline{s_c} \gg 1 \tag{93}$$

$$\overline{s_c} \gg c_0 \tag{94}$$

5 Kinetic behaviour

This section describes the kinetic process leading to the formation of the Scw and Dpp gradient. As described in the paper, the shuttling of Scw by the diffusible Sog-Scw complex into the dorsal-most region is the main mechanism underlying Scw gradient formation. The figures below illustrate this process. Fig. 1 presents the evolution of Scw and Dpp profiles for a time series. Although the profile near the midline is still developing after 60 min., the profile at the threshold (x=0.5) reaches a steady state much earlier, As can be seen in Fig. 2.

In section 2.1 we show that the steady state profile of Scw is highly robust to changes in the parameters. What we find analytically and numerically is that the dynamics of the system varies considerably with the parameters. Below we estimate analytically that the steady-state time is of the order:

$$t_R \approx \frac{\overline{s_c}\lambda T}{\eta_s D_c} l_1^2 = \frac{\overline{s_c}}{c_0}\tau_{diff} > \tau_{diff}, \tag{95}$$

here, τ_{diff} is the diffusion time of the Sog-Scw complex across the dorsal region. Fig. 3 compares the dynamic behaviour of different parameters. As can be seen, in the Sog hetrozygous case it takes almost twice the time to reach staedy state at $x = 0.5$, than in the wild-type case. In the case of Tld or Scw it doesn't take half the time since the production time scale (taken to be 10 minutes in our simulations) dictates a minimum patterning time.

5.1 Analytic approximation of the shuttling time.

In this section we provide an analytic estimate for the shuttling time of the ligand to the dorsal midline. Based on simulation results we have looked for a wavelike solution for the system Eqs. 2-4. Specifically, we look for a solution of the form:

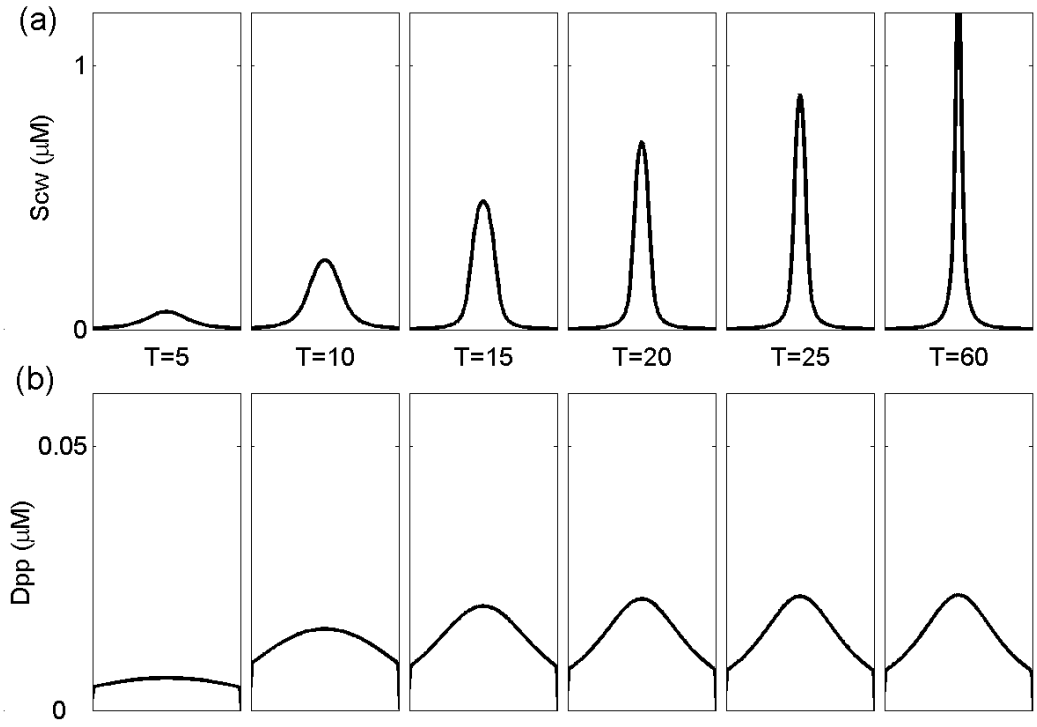

Figure 1: The profile of Scw and Dpp for the indicated times (in minutes).

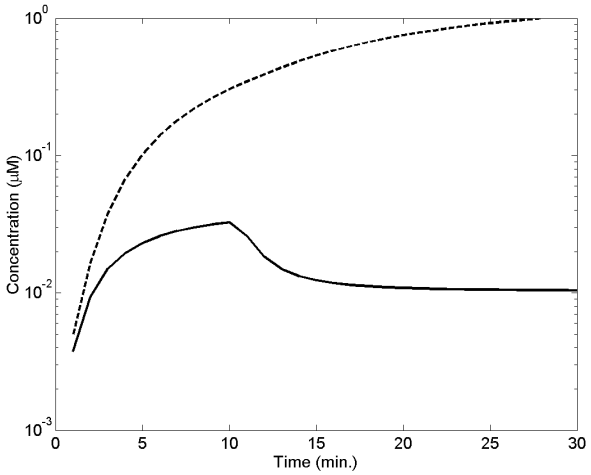

Figure 2: The concentration level of Scw at $x = 0.5$ (full line) and $x = 0$ (dashed line) as a function of time. The break in the full line is at the time when production of Scw is terminated.

$$s(x,t) = t^{-m}\hat{s}(u)\theta(u) \tag{96}$$

$$c(x,t) = t^{-m}\hat{c}(u)\theta(u) \qquad u = gt^m - x \tag{97}$$

$$s_c(x,t) = \hat{s}_c(u)\theta(u), \tag{98}$$

where g and m define the wave "velocity". The origin, $x = 0$, is defined here at the boundary between the dorsal and neural ectoderm, where Sog is being produced. We are looking for a finite solution in the region $gt^m \geq u \geq 0$ ($gt^m \geq x \geq 0$). Substituting the functional forms, Eqs. 96-98, into Eqs. 2-4, we find:

$$-mt^{-m-1}\hat{s}(u) + mgt^{-1}\frac{d\hat{s}}{du} = t^{-m}(D_s\nabla^2\hat{s} - k_b\hat{s}\hat{s}_c) \tag{99}$$

$$-mt^{-m-1}\hat{c}(u) + mgt^{-1}\frac{d\hat{c}}{du} = t^{-m}(D_c\nabla^2\hat{c} + k_b\hat{s}\hat{s}_c - \lambda T\hat{c})mgt^{m-1} \tag{100}$$

$$mgt^{m-1}\frac{d\hat{s}_c}{du} = t^{-m}(-k_b\hat{s}\hat{s}_c + \lambda T\hat{c}). \tag{101}$$

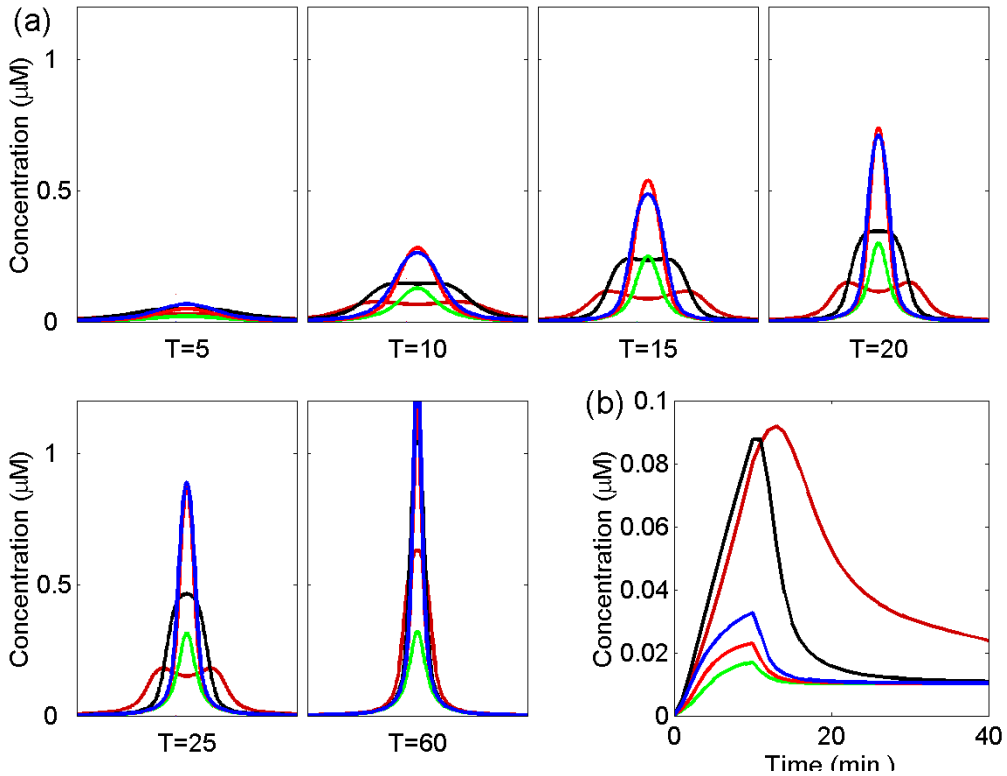

Figure 3: (a) Scw profiles at different times for the reference system (blue), Tld overexpression (dark red) and Sog (black), Scw (green) and Tld (red) hetrozygous systems.

At long times, $t \gg 1$ we can ignore the t^{-1}, t^{--m-1} terms obtaining the quasi steady state equation:

$$0 = D_s \nabla^2 \hat{s} - k_b \hat{s} \hat{s}_c \tag{102}$$

$$0 = D_c \nabla^2 \hat{c} + k_b \hat{s} \hat{s}_c - \lambda T \hat{c} \tag{103}$$

$$mg \frac{\partial \hat{s}_c}{\partial u} t^{2m-1} = -k_b \hat{s} \hat{s}_c + \lambda T \hat{c}. \tag{104}$$

If $m < 0.5$ (or for large enough u when $m = 0.5$), we can neglect the term $\frac{g}{2} \frac{\partial \hat{s}_c}{\partial u} t^{2m-1}$ on the LHS of Eq. 104. In this region, Eqs. 102-103 are reduced to the steady state system Eqs. 5-7. The solution in this region is thus given by Eqs. 15-17:

$$s = \frac{\eta_s}{2D_s}(u^2 + \varepsilon^2) \tag{105}$$

$$c = c_0 = \frac{\eta_s}{\lambda T g} \tag{106}$$

$$s_c = \frac{l_b^2}{u^2 + \varepsilon^2} \qquad ; \qquad \varepsilon \simeq \frac{\pi/2}{s_c^{tot}}. \tag{107}$$

As can be seen from the solution for the ligand, the ligand profile is very steep near the edge where most of it is concentrated in the limited region of size ε. Further away the profile is robust to the specific amount of the ligand. The wave velocity g and the appropriate power of time m, are found by solving the equations at the boundary of the wave, $u \sim 0$. An approximated solution can be found by noting that for $\varepsilon \longrightarrow 0$, s_c behaves as a dirac δ function:

$$\hat{c}(u) = \frac{\eta_s}{\lambda T g} \theta(u) \tag{108}$$

$$\hat{s}_c(u) = s_c^{tot}(t) \delta(u). \tag{109}$$

Adding equations 103,104 we obtain:

$$mg \frac{\partial \hat{s}_c}{\partial u} t^{2m-1} = D_c \nabla^2 \hat{c}, \tag{110}$$

and by using the above approximation:

$$mg s_c^{tot}(t) t^{2m-1} \delta'(x) = D_c \frac{\eta_s}{\lambda T g} \delta'(x). \tag{111}$$

We distinguish here between two cases. In the first, all ligand is concentrated on the boundary of the dorsal region and there is no ligand on the other side of the wave. In this case, total ligand amount is conserved as the wave advances, $s_c^{tot}(t) = s_c^{tot}$. Eq. 111 will be valid if:

$$g^2 = 2\frac{D_c \eta_s}{s_c^{tot} \lambda T} \qquad ; \qquad m = \frac{1}{2}. \tag{112}$$

On the second case, the ligand is distributed evenly along the region and the wave advances in a region with constant concentration of the ligand. In this case the amount of ligand is proportional to the distance passed by the wave, gt^m; $s_c^{tot}(t) = \frac{s_c^{tot}}{l_1} gt^m$, where l_1 is the length of the region. Under these conditions the appropriate values for g and m are:

$$g^3 = \frac{3\eta_s l_1 D_c}{s_c^{tot} \lambda T} \qquad ; \qquad m = \frac{1}{3}. \tag{113}$$

The system will reach steady state only when the peak has reached the midline ($x = l_1$), this will happen after a time t_R in the first case:

$$t_R \approx \left(\frac{l_1}{g}\right)^2 = \frac{s_c^{tot} \lambda T}{2 D_c \eta_s} l_1^2 = \frac{1}{2}\frac{s_c^{tot}}{c_0}\tau_{diff}, \tag{114}$$

and a time t'_R on the second case:

$$t'_R \approx \left(\frac{l_1}{g}\right)^3 = \frac{s_c^{tot} \lambda T}{3 D_c \eta_s} l_1^2 = \frac{1}{3}\frac{s_c^{tot}}{c_0}\tau_{diff} = \frac{2}{3} t_R, \tag{115}$$

where we have defined $\tau_{diff} = \frac{l_1^2}{D_c}$ to be the characteristic diffusion time of the complex. The second robustness condition $s_c^{tot} \gg c_0$ implies that the more robust the system, the longer it takes to reach the steady state. For the reference parameters used in the simulations, we find that $t_R \simeq 5T_{diff}$ which is in good agreement with the numerical results. Simulation results confirm the scaling laws, and the wave velocity given by Eqs. 114,115. The validity of the above approximation is true for cases where a step like wave solution exists. This situation is typical for relatively high values of λ and η such that the degradation length scale is smaller than the system's length scale, l_1; $l_d \equiv \sqrt{\frac{D_s}{\lambda T}} < l_1$ lower levels will lead to longer times. This approximation

is good for the chosen reference system. Since Scw is produced both within and outside of the dorsal region, the dynamical behavior of the system is a combination of the two conditions and the dependence of g on parameters is an intermediate dependence as well (Eqs. 112,113).

For small enough α we find that $t_\alpha(x) \simeq t_R$. The above approximation is not good for regions where $x \simeq \varepsilon$ where patterning is much slower.

6 Linear deviations from precise robustness

6.1 Scw diffusion

In box 1 we assumed that Scw couldn't diffuse. Numerically we find that if Scw diffusion; D_{sc}, is small compared D_s, the deviations from precise robustness are small, as illustrated in figure 4a,b,c below. Defining $D^0_{sc\ 5\%}$ to be the diffusion rate for which the threshold moves 5% outward of its location when $D_{sc} = 0$, we find that for the reference system used in the paper $D^0_{sc\ 5\%} \approx 7 \cdot 10^{-4} \left(\frac{D_c}{D^0_c}\right)^{0.5} \left(\frac{\eta_s}{\eta^0_s}\right)^{1.15} \left(\frac{T}{T^0}\right)^{-2/3} \left(\frac{\overline{s_c}}{\overline{s^0_c}}\right)^{-1.3} D_s$. The dependence of $D^0_{sc\ 5\%}$on the system's parameters is shown in figure 4d.

6.2 Scw production and degradation

The limited production or degradation of Scw does not alter the robustness as long as the shuttling mechanism is fast enough compared to the production or degradation time scales. In figure 5 we examine a model in which Scw is constantly being produced and degraded at rates η_{sc} and α_{sc}, respectively. We assume that a constant steady state Scw amount $\overline{s_c} = \eta_{sc}/\alpha_{sc}$ is maintained. Defining $\alpha^0_{sc\ 5\%}$ as the degradation rate for which the threshold position is moved 5% outward of its location when $\alpha_{sc} = 0$, we find that below a characteristic degradation rate (or production rate), robustness is retained. We find the characteristic degradation rate to be $\alpha^0_{sc\ 5\%} \approx 4 \cdot 10^{-3} \left(\frac{D_c}{D^0_c}\right)^{0.8} \left(\frac{\eta_s}{\eta^0_s}\right)^{1} \left(\frac{T}{T^0}\right)^{-0.8} \left(\frac{\overline{s_c}}{\overline{s^0_c}}\right)^{-1} \tau^{-1}_{diff}$.

6.3 Free Sog degradation

A linear (or other form of) degradation of *free* Sog change the steady state solution in two ways; Inside the dorsal region it sharpen the profiles of Sog

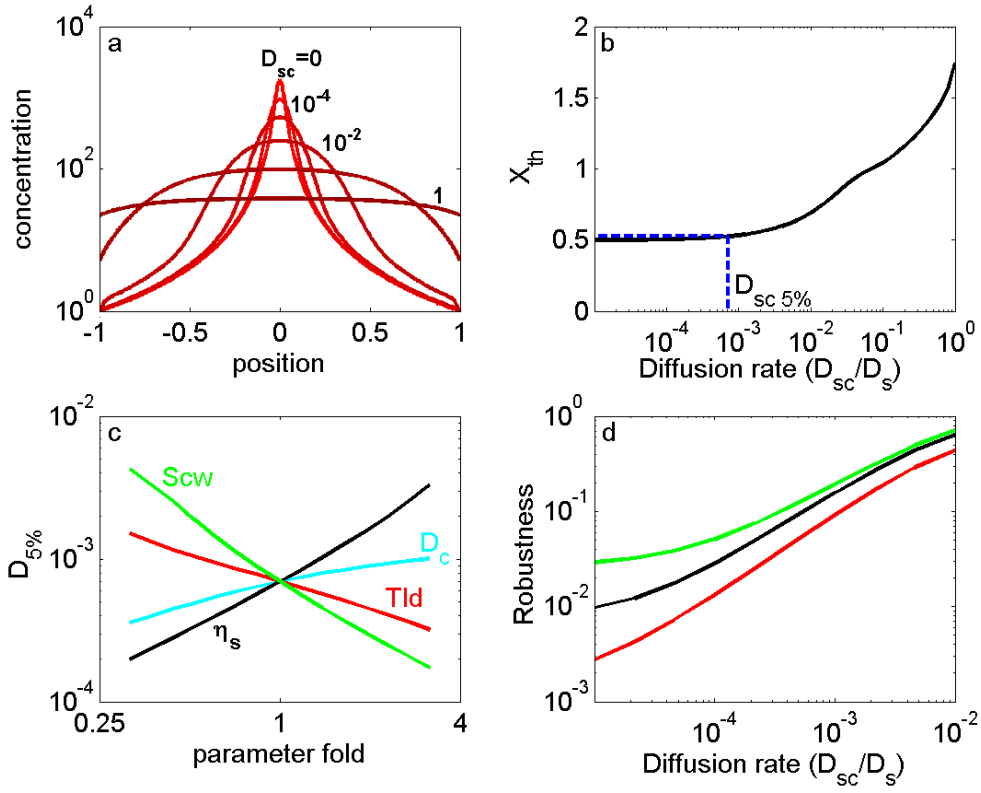

Figure 4: (a) The Scw concentration profile for $D_{sc} = 0$ and for 4 orders of magnitude of D_{sc} (the value of the diffusion constant, are given as the ratio D_{sc}/D_s). (b) Position of the threshold as a function of D_{sc}. $D^0_{sc\ 5\%}$ is indicated. (c) The value of $D^0_{sc\ 5\%}$ as a function of the parameters Sog (black), Tld (red), Scw (green) and the complex diffusion constant (cyan) (d) The change in robustness of the system for moderate values of D_{sc}. Robustness is measured as the change of position of the threshold (in percents) across an order of magnitude around the reference system. Parameters are indicated with same colors as in **c**.

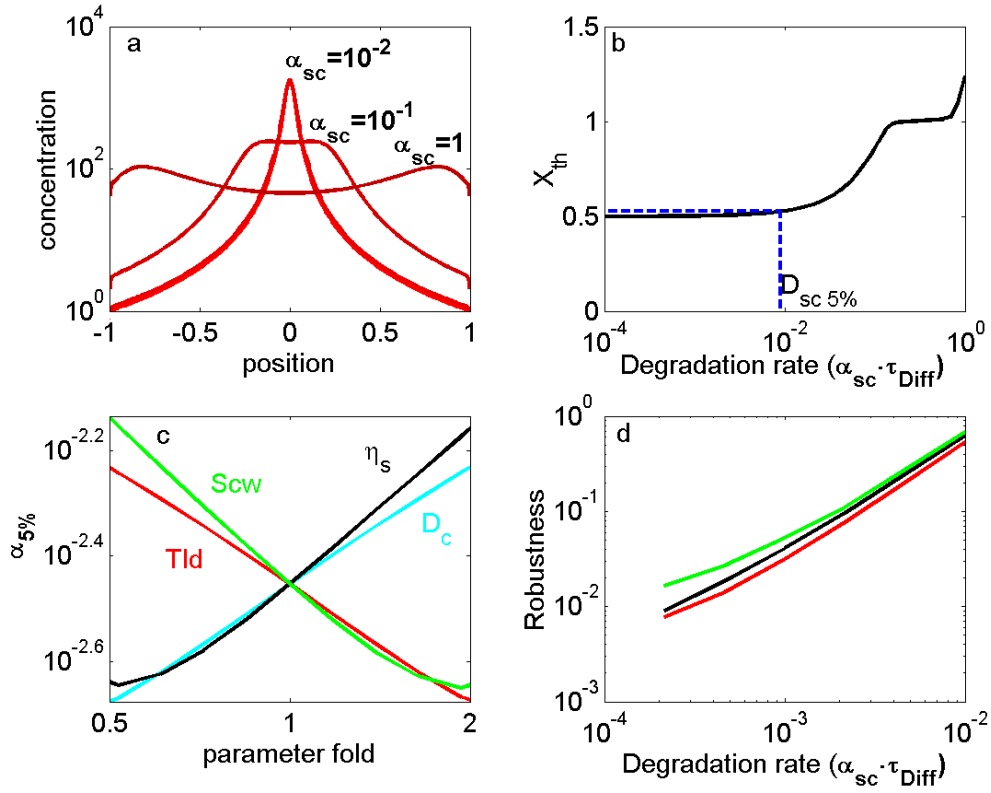

Figure 5: (a) The Scw concentration profile for 3 different values of α_{sc} (measured in units of $1/\tau_{diff}$(b) position of the threshold as a function of α_{sc} in units of $1/\tau_{diff}$, where τ_{diff} is the diffusion time acrros the dorsal region. $\alpha^0_{sc\ 5\%}$ (defined as $D^0_{sc\ 5\%}$) is indicated. (c) The value of $\alpha^0_{sc\ 5\%}$ as a function of the four parameters indicated in the figure.

and Scw, while outside of the dorsal region it serves to reduce the effective incoming Sog flux.

If we assume Sog is degrading linearly with a constant γ, The steady-state equation for Sog inside the dorsal region, (Eq. 8), turns into:

$$D_s \nabla^2 s - \lambda T c_0 - \gamma s = 0. \tag{116}$$

The contribution of the linear degradation term will be negligible if $\lambda T c_0 \gg \gamma s$ for all s:

$$\lambda T c_0 \gg \gamma s_{\max} \approx \gamma \frac{\lambda T c_0}{2 D_s} l_1^2. \tag{117}$$

This implies that the linear degradation time scale should be much slower than the diffusion time scale (or that the linear degradation length scale should be larger than the system's length scale):

$$\tau_{\deg} = \gamma^{-1} \gg \frac{l_1^2}{D_s} = \tau_{diff} \qquad \Leftrightarrow \qquad L_{\deg} = \sqrt{\frac{D_s}{\gamma}} \gg l_1, \tag{118}$$

where we used Eqs. 16 to determine the maximum value of Sog (at the dorsal boundary). In such a case, the profiles will retain their form and robustness. It can be shown that the shape of Scw profile will be altered for higher values of γ, but the robustness of the profile to Scw, Tld or Sog concentrations will be retained. On the other hand, the profile will not be robust to changes in the value of γ. In figure 6a,d we show simulations results of the the simple model including the region outside of the dorsal ectoderm. As can be seen, the threshold position and its robustness are not altered considerbly even at rather high degradation rates.

The other effect of free Sog degradation is to change the boundary conditions on Sog flux by reducing the amount of Sog available for the shuttling process outside the dorsal region. We define the Sog flux, η_{eff}, as the flux of Sog degraded through the complex Sog-Scw:

$$\eta_{eff} = \lambda T c_0. \tag{119}$$

For high values of γ we find that most of Sog flux can be degraded by linear degradation (i.e. $\eta_{eff}/\eta_s \ll 1$), while the system retains its robust profile

(compare Figs. 6a and 6c). The increase of γ elevates considerably the time to reach steady state (see 6b). This is mostly due to the reduction in effective Sog flux, if the effective flux is being kept constant as γ increases (by increasing the total flux), the time is kept almost constnat (not shown).

The full model (Eqs. 1a-k) includes a linear degradation term for Sog - Its binding process to Tsg. We can deduce from the above discussion that the flux of Sog degraded by interaction with Tsg/Dpp can be on the same order of magnitude as the flux of Sog degraded by interaction with Scw without considerably altering the shapes and robustness of the profile of Scw. For the chosen reference system the ratio of the fluxes is about 1:1. Note that in a case where $\eta_{eff}/\eta_s \ll 1$, a *dpp* homozygous mutant embryo might loose the Sog profile since the Scw system will be overwhelmed by Sog flux (see section 4).

7 Non-Robust mechanisms

7.1 Non-robustness of a simple inhibitory model

Here we give an analytic solution for an example of a family of models in which Sog behaves mostly as an inhibtor of the Activation and not as a shuttling agent. We Assume that Tld degrades free Sog and that Scw can bind as well as dissociate from Sog. We also assume that neither Scw, nor the complex can diffuse. This system is described by the following equations:

$$\frac{\partial s}{\partial t} = D_s \nabla^2 s - k_b s s_c + k_{-b} c - \lambda T s \tag{120}$$

$$\frac{\partial c}{\partial t} = k_b s s_c - k_{-b} c \tag{121}$$

$$s_c^{tot} = s_c + c. \tag{122}$$

Using Eqs. 121, 122 we find the binding formula for Scw and the complex:

$$s_c = \frac{k_{-b}/k_b}{s + k_{-b}/k_b} s_c^{tot}; \qquad c = \frac{s}{s + k_{-b}/k_b} s_c^{tot}. \tag{123}$$

Adding Eqs. 120, 122 we get:

$$\frac{\partial s}{\partial t} = D_s \nabla^2 s - \lambda T s, \tag{124}$$

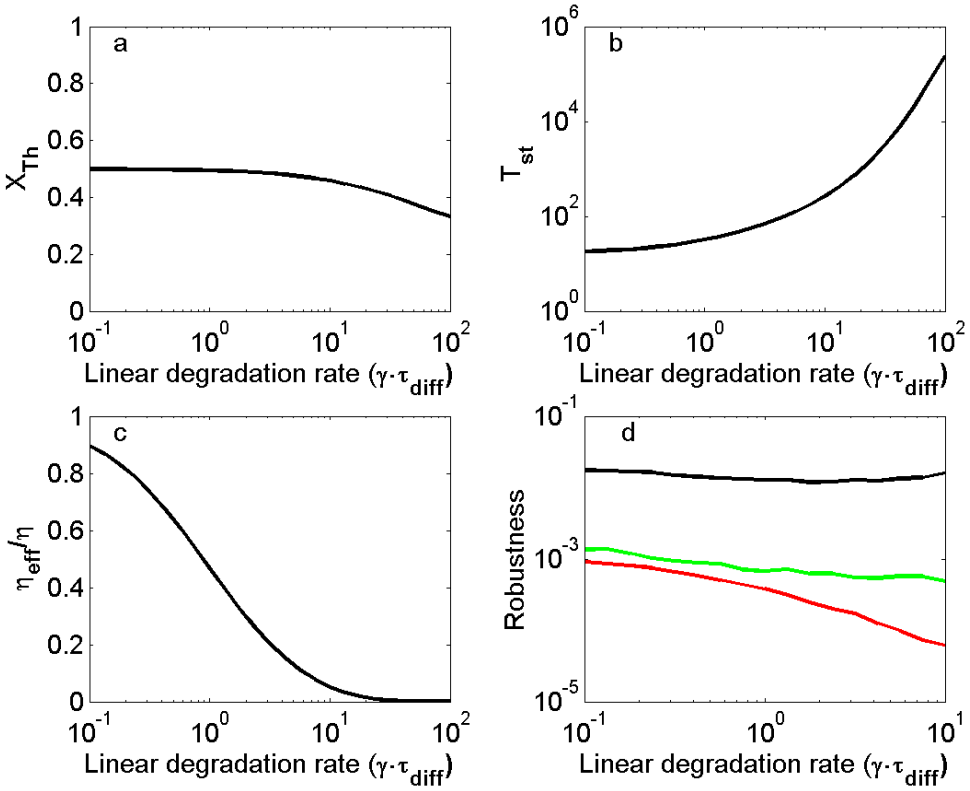

Figure 6: Response of the system as a function of the linear degradation rate of Sog. (a) The threshold position.The threshold is defined to give $X_{Th} = 0.5l_1$ for $\gamma = 0$. (b) The time to reach steady state. (c) The effective Sog rate. (d) Robustness of the system to Sog (black), Scw (green) and Tld (red).

with the solution:

$$s \simeq s_0 \cosh(x/\sqrt{\frac{D_s}{\lambda T}}). \tag{125}$$

The expression for Scw is:

$$s_c = \frac{k_{-b}/k_b}{s_0 \cosh(x/\sqrt{\frac{D_s}{\lambda T}}) + k_{-b}/k_b} s_c^{tot}. \tag{126}$$

As can be clearly seen, $s_c(x)$ is linearly dependent on s_c^{tot} and s_0, and has a length scale which is defined by Tld. This expression is highly non-robust.

7.2 Direct competition between Scw and Dpp on Sog will lead to a non-robust mechanism

In this section we show that neglecting Tsg contribution by assuming a direct interaction between Dpp and Sog/Tld in an identical fashion to Scw's interaction will lead to a non-robust model. We can write the following equations to describe the system:

$$\frac{\partial s}{\partial t} = D_s \nabla^2 s - k_b^{(1)} s s_c - k_b^{(2)} s d_p \tag{127}$$

$$\frac{\partial c_1}{\partial t} = D_{c1} \nabla^2 c_1 + k_b^{(1)} s s_c - \lambda_1 T c_1 \tag{128}$$

$$\frac{\partial s_c}{\partial t} = -k_b^{(1)} s s_c + \lambda_1 T c_1 \tag{129}$$

$$\frac{\partial c_2}{\partial t} = D_{c2} \nabla^2 c_2 + k_b^{(2)} s d_p - \lambda_2 T c_2 \tag{130}$$

$$\frac{\partial d_p}{\partial t} = -k_b^{(2)} s d_p + \lambda_2 T c_2 \tag{131}$$

In steady state we find (in a similar fashion to the analysis above) that:

$$c_1 = c_1^0; \qquad c_2 = c_2^0 \tag{132}$$

$$s = \frac{1}{2}(\lambda_1 T c_1^0 + \lambda_2 T c_2^0)(x^2 + \varepsilon^2) \tag{133}$$

$$s_c = \alpha \cdot \frac{2D_s/k_b^{(1)}}{x^2 + \varepsilon^2}; \qquad \alpha = \frac{\lambda_1 T c_1^0}{(\lambda_1 T c_1^0 + \lambda_2 T c_2^0)} \tag{134}$$

$$d_p = (1 - \alpha) \cdot \frac{2D_s/k_b^{(2)}}{x^2 + \varepsilon^2} \tag{135}$$

The conservation condition on Scw and Dpp implies that:

$$\overline{s_c} = \frac{2D_s}{k_b^{(1)}} \alpha \int \frac{dx}{x^2 + \varepsilon^2} \tag{136}$$

$$\overline{d_p} = \frac{2D_s}{k_b^{(2)}} (1 - \alpha) \int \frac{dx}{x^2 + \varepsilon^2}. \tag{137}$$

Dividing the two conditions we get:

$$\frac{\alpha}{1 - \alpha} = \frac{k_b^{(1)} \overline{s_c}}{k_b^{(2)} \overline{d_p}}. \tag{138}$$

The competition term α, will give a linear ratio term in the expression for one of the components:

$$s_c = \frac{2D_s/k_b^{(1)}}{x^2 + \varepsilon^2} (1 + \frac{k_b^{(2)} \overline{d_p}}{k_b^{(1)} \overline{s_c}})^{-1}; \qquad d_p = \frac{2D_s/k_b^{(2)}}{x^2 + \varepsilon^2} (1 + \frac{k_b^{(1)} \overline{s_c}}{k_b^{(2)} \overline{d_p}})^{-1} \tag{139}$$

This will lead to non-robustness of at least one of the profiles to Scw concentration.